Automating the assessment of wrist motion in telerehabilitation with haptic devices

Roni Barak Ventura^{a,b}, Angelo Catalano^{b,c}, Rayan Succar^{a,b}, and Maurizio Porfiri*^{a,b,d}

- ^aCenter for Urban Science and Progress, New York University Tandon School of Engineering, 370 Jay Street, Brooklyn, NY 11201, USA
- ^bDepartment of Mechanical and Aerospace Engineering, New York University Tandon School of Engineering, 6 MetroTech Center, Brooklyn, NY 11201, USA
- ^cDipartimento di Meccanica, Matematica e Management, Politecnico di Bari, Via Orabona 4, Bari, 70125, Italy
- ^dDepartment of Biomedical Engineering, New York University Tandon School of Engineering, 6 MetroTech Center, Brooklyn, NY 11201, USA

ABSTRACT

Stroke-induced motor impairment often prevents survivors from participating in activities of daily living, adversely impacting their quality of life. Desktop delta robots such as the Novint Falcon have been utilized in various home-settings to help recover fine-motor skills. They are compact and affordable, and can provide programmable sensorimotor feedback. In spite of these favorable features, it is presently not possible to directly measure the user's wrist angles while interacting with these robots, which undermines their prospective use in telerehabilitation as patients' motor performance cannot be reliably assessed. Here, we propose an experimental set-up where patients strap a smartphone device to their forearm and manipulate a haptic robot. In this setting, data from inertial sensors embedded in the smartphone will be integrated with data from the robot in a classification algorithm that infers the wrist angle. To study the viability of this approach, we perform experiments with one healthy user. We fix two inertial measurement units on their body, one on their forearm and one on the back of their hand, to measure the true wrist angle as they perform a motor task with a Novint Falcon device. We train a machine learning algorithm that predicts wrist angles from a single wearable sensor and the Novint Falcon movements. This effort constitutes a step toward automatic assessment of wrist movements in fine motor telerehabilitation and could enable real-time feedback in the absence of a therapist.

Keywords: Data science, delta robots, machine learning, motion analysis, stroke rehabilitation

1. INTRODUCTION

Stroke is a leading cause of adult disability in the United States, where approximately 795,000 people experience a new or recurrent stroke every year.¹ A significant portion of stroke survivors experience debilitating impairments in fine motor skills,² which are essential for tasks involving muscles in the hands and wrists such as writing, turning pages, eating, and using computer keyboards. Rehabilitation therapy focusing on fine motor skills is critical for restoring patients' independence and improving their quality of life.³ However, in order to maximize recovery, patients must adhere to a therapy regimen consisting of high-intensity, high-frequency exercise routines. Since standard physical therapy requires the time commitment and physical engagement of both patients and therapist,⁴ most patients do not receive sufficient treatment for full recovery.

Telerehabilitation, or the provision of rehabilitation services over telecommunication networks to patients' homes, presents a promising approach to facilitate frequent and accessible therapy. Several robots were designed to relay interactive, reprogrammable, and reproducible treatment to patients,⁵ and for wrist rehabilitation in particular.^{6,7} For example, a wrist extension was developed for the MIT Manus, a robot that is considered a

M.P.: Email:mporfiri@nyu.edu, Telephone: 1 646 997 3681

^{*}Further author information: (Send correspondence to M.P.)

benchmark for programmed upper limb treatment.⁸ Similarly, the Rutgers Master II,^{9,10} IIT Genova,³ UTM,¹¹ Haptic Knob,¹² and REHA¹³ were designed to recover intricate fine motor skills. While robotic devices offer tailored treatment, their adoption is hindered by several limitations, including their physical size, the need for specialized knowledge for operation, and prohibitive cost.¹⁴

In the search for affordable and user-friendly alternatives, low-cost gaming devices have emerged as potential tools for wrist rehabilitation. 15,16 One such device is the Novint Falcon, a desktop delta robot that is also used as a game controller (Figure 1a). The Novint Falcon affords translational hand movement within a workspace of $101.6 \text{ mm} \times 101.6 \text{ mm} \times 101.6 \text{ mm} (4'' \times 4'' \times 4'')$ (Figure 1a). It is capable of measuring the end-effector's trajectory with remarkable temporal and spatial resolutions, 17,18 and offers remotely programmed force feedback with the widest range among commercially available devices, 19 reaching a maximum force of $8.8 \text{N}.^{17,18}$ The Novint Falcon's force field can be applied to assist movement training 17 and simultaneously measure the forces applied by the hand 20 or finger-tip, 21 thereby providing important information for the assessment of fine motor performance. $^{15,17,22-24}$

Despite its many advantages, the Novint Falcon has a significant limitation: it cannot measure movement of the user's wrist, which is critical for reliable evaluation by therapists remotely. To address this limitation, we propose a set-up where patients strap a smartphone device to their forearm and manipulate the Novint Falcon (Figure 1b). We anticipate that additional information on the forearm's orientation and velocity (which can be readily drawn from sensors inherently embedded in the smartphone) could be combined with data from the Novint Falcon to infer the user's wrist angles. Since the wrist angle is not directly measured in this set-up, a machine learning algorithm can be developed to predict the wrist angle.

In this paper, we explore the usability of our proposed approach. We collected data from a single, healthy individual who interacted with the Novint Falcon. In order to accurately measure the subject's actual, ground-truth wrist angle throughout the interaction, two Inertial Measurement Units (IMUs) were attached to her upper limb. One IMU was placed on her forearm and another was placed on the back of her hand (Figure 1c). Data from both IMUs is used to calculate the true wrist angle. Data from the IMU that is strapped to the forearm is also used as a substitute for a phone that would be strapped on her forearm. We train a linear regression model that integrates data from this IMU with data from the Novint Falcon to predict the wrist angles. Our analysis is conducted with a specific focus on the wrist pitch, as it constitutes the majority of the degrees of freedom in the wrist movement.^{25,26} We present some preliminary results, which constitute a step toward automatic assessment of wrist movements in fine motor telerehabilitation.

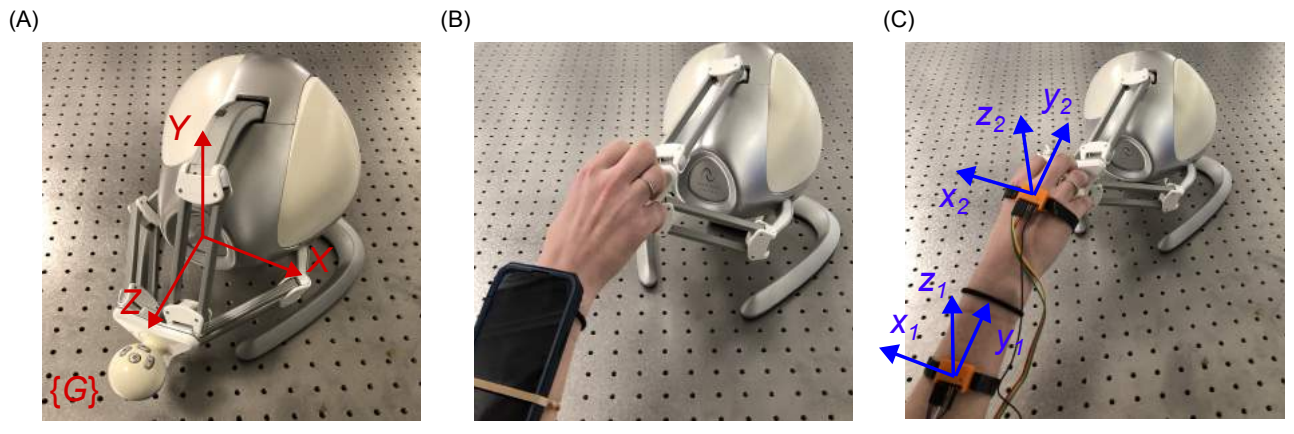


Figure 1: The Novint Falcon, a compact and affordable desktop delta robot. (A) The game controller with overlaid global coordinate system $\{G\}$, measuring the end-effector's motion in three dimensions (X, Y, and Z). (B) Illustration of our proposed telerehabilitation set-up, where a user straps a smartphone to their forearm and manipulates the end-effector. (C) Illustration of our experimental set-up where the subject wears two IMUs, one on the forearm and another on the back of the hand, to measure the wrist angle. The local reference frame of each IMU is overlaid in blue.

2. METHODS

2.1 Data collection

We gathered data on a single, healthy subject who interacted with the Novint Falcon. Two IMUs (MPU-6050, InvenSense Inc., Sunnyvale, California) were fixed in 3D-printed housings and strapped onto the first author's limb with an elastic drawstring. One IMU was placed on the dorsal side of her forearm and the other was placed on the dorsum of her hand. She interacted with the Novint Falcon in a citizen science-based game that was developed for a previous study with the device.²⁷

During this exercise, two datasets were generated. The first dataset recorded the position of the Novint Falcon's end effector in three dimensions (X, Y, Z) with respect to global frame G (Table 1). The second dataset logged the output of the two IMUs. For clarity, the IMU placed on the forearm and its output are denoted with a subscript of 1, and the IMU placed on the hand and its output will be denoted with a subscript of 2. From the gyroscope, each IMU recorded its orientation relative to G in Tait-Bryan angles (yaw about the z-axis of the sensor, α_1 and α_2 ; pitch about the y-axis of the sensor, β_1 and β_2 ; and roll about the x-axis of the sensor, γ_1 and γ_2) and angular velocities about the same axes $(\omega_{1,z}, \omega_{2,z}, \omega_{1,y}, \omega_{2,y}, \omega_{1,x},$ and $\omega_{2,x}$). From the accelerometer, the x-,y-, and z-components of the gravity vector were logged $(g_{1,x}, g_{2,x}, g_{1,y}, g_{2,y}, g_{1,z},$ and $g_{2,z}$). All measurements are summarized in Table 1.

All three datasets were collected simultaneously. Novint Falcon data were collected at a sampling rate of 45 measurements per second whereas IMU data were collected at a sampling rate of 13 measurements per second.

Sensor	Variable	Notation
Novint Falcon	position on the X-axis	X
	position on the Y-axis	Y
	position on the Z-axis	Z
IMU_1	roll angle about x	γ_1
	pitch angle about y	eta_1
	yaw angle about z	α_1
	angular velocity about x	$\omega_{1,x}$
	angular velocity about y	$\omega_{1,y}$
	angular velocity about z	$\omega_{1,z}$
	x component of the gravity vector	$g_{1,x}$
	y component of the gravity vector	$g_{1,y}$
	z component of the gravity vector	$g_{1,z}$
IMU_2	roll angle	γ_2
	pitch angle	eta_2
	yaw angle	α_2
	angular velocity about x	$\omega_{2,x}$
	angular velocity about y	$\omega_{2,y}$
	angular velocity about z	$\omega_{2,z}$
	x component of the gravity vector	$g_{2,x}$
	y component of the gravity vector	$g_{2,y}$
	z component of the gravity vector	$g_{2,z}$

Table 1: Summary of the variables collected by the Novint Falcon and IMUs.

2.2 Data processing

Data were processed in MATLAB (MATLAB R2023b, The MathWorks, Inc., Natick, MA, USA). First, the wrist angles the subject assumed throughout the activity were inferred from IMU data for every measurement sampled. Specifically, the Tait–Bryan angles in each IMU were organized into quaternion representations. Then, the quaternion associated with IMU_1 was multiplied by the conjugate of the quaternion associated with IMU_2 to obtain their relative orientations.

After computing instantaneous wrist angles, we synchronized the measurements made by the Novint Falcon and the IMUs in Python using pandas (version 1.4.2). We identified the largest time difference between consecutive samples and divided each time series into intervals of that size so that every interval contains at least one measurement. Since each sensor recorded measurements at a different sampling rate, intervals for one sensor contained more measurements than the intervals of another. The entire interval was replaced by the average of measurements it contained to obtain an equal number of observations along all time series.

2.3 Training a machine learning algorithm

A linear regression model was trained in Python using the scikit-learn (version 1.0.2) and statsmodels (version 0.13.2) libraries. We aimed to predict wrist angles a user assumes from measurements made by the Novint Falcon and IMU_1 . Therefore, the relative angles we computed between the IMU_3 were input as the true wrist angle measurements. The 12 variables recorded from the Novint Falcon and IMU_1 (which could be measured by a phone strapped to the forearm) were included as potential predictors in the model. Training was carried out on the first 70% of the measurements, reserving the remaining 30% to avoid overfitting.

Since movements trajectories are autoregressive in nature²⁸ (that is, the state of postures informs on future states of postures), we also considered the predictive value of lagged time series. To determine the number of lags that would be relevant for training, we embedded the time series of each of the 12 predictive variables by a number of time steps ranging from zero to ten time steps (corresponding to lags ranging from zero to three seconds). We trained eleven linear regression models, gradually increasing the number of lagged variables that are included among the predictive variables. For example, when we trained a model with two lags, the original 12 predictive variables were considered along with their lagged variants such that the training set contained 36 time series in total. Similarly, when all ten lags were considered, the model was trained on a maximum of 132 predictive variables. For each model, we computed the mean squared error (MSE) using the 30% out-of-sample measurements and Akaike information criterion (AIC) using all measurements.

We selected the model with the number of lags that minimizes MSE and AIC, and further assessed its performance through the R-squared (R^2) . To evaluate the importance of each predictor, the model was fitted with z-standardized time series and the absolute values of coefficients were examined.

3. RESULTS

3.1 Data collection and processing

The subject interacted with the Novint Falcon for a total of 199 seconds. The raw time series contained 8,741 observations for the Novint Falcon and 2,598 observations for both IMUs. After synchronization, the time series were reduced to 664 observations.

3.2 Training a machine learning algorithm

Comparison of the eleven linear regression models revealed that the MSE is minimized when time series with six time lags are included in the training set (Figure 2). With respect to the AIC score, the model performs best when five lags are included in training.

The model trained with 72 time series (five lags) was selected as it minimized both MSE and AIC. The model demonstrated exceptional goodness-of-fit, with a coefficient of determination $R^2 = 0.916$ (Figure 3). Inspection of the coefficients of its predictors showed that Y, β_1 , α_1 , $\omega_{1,x}$, and $\omega_{1,z}$ contributed the most to the model (Figure 4). In particular, β_1 was the most predictive variable, as well as α_1 , $\omega_{1,x}$, and γ_1 . A lag of zero was most informative among those variables, as well as Y. β_1 and $g_{1,x}$ contributed to the fit when a lag of four time steps was imposed on them. In contrast, Z, $\omega_{1,z}$, $\omega_{1,y}$, and X were least informative for the model.

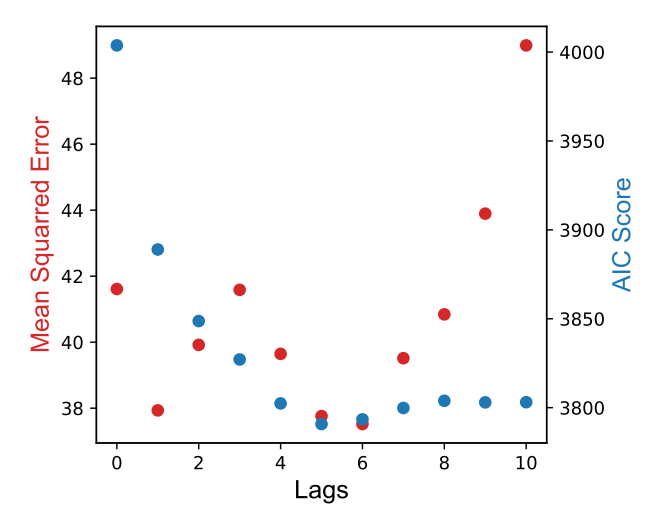


Figure 2: Evaluation of autoregression in the subject's motion. Eleven linear regression models were trained on data sets with lags ranging from zero to ten. Red markers indicate the MSE of each model whereas blue markers indicate their AIC scores.

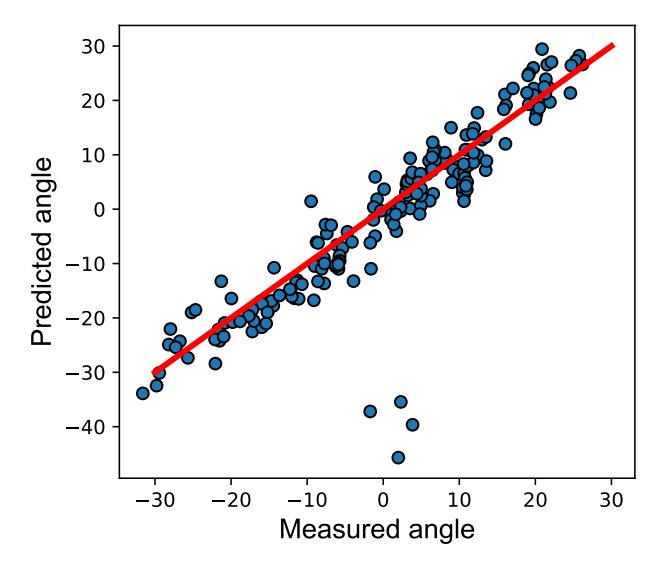


Figure 3: Linear fit of the measured wrist angles against the predicted ones.

4. DISCUSSION

This study explores the possibility of predicting the hand posture of patients undergoing fine motor telerehabilitation with haptic devices. Currently, remote assessment of patients who are interacting with haptic devices by healthcare providers is not feasible, severely undermining their prospective use in home-based rehabilitation. To overcome this challenge, we propose the integration of haptic devices with smartphones and machine learning algorithms to quantify patients' fine motor performance during telerehabilitation exercises. In particular, we envision patients strapping a smartphone to the forearm of their affected limb and interacting with haptic devices. Within this simple set-up, data from IMUs that are inherently embedded in smart devices could complement data on the trajectory of the end effector the patient is manipulating to predict their wrist angle throughout a prescribed physical activity. Highly resolved measurements of wrist movement could not only support remote assessment of motor performance, but also enable real-time feedback systems that prompt the patient to correct movements and behaviors.

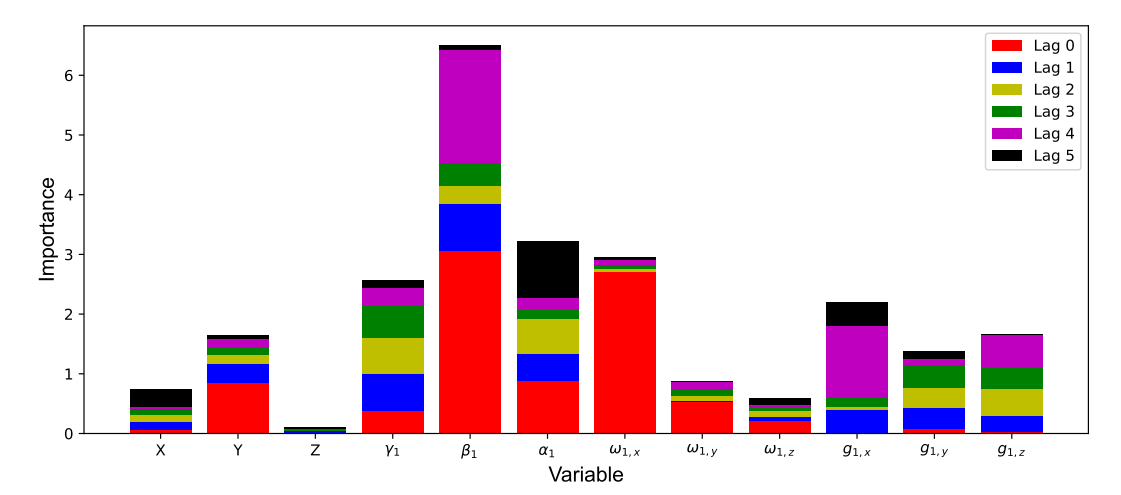


Figure 4: Importance of each variable for the model fit from the associated coefficients.

In the present study, we explore the feasibility of the proposed approach with the Novint Falcon, a low cost delta robot that was studied extensively for its prospective use in fine motor rehabilitation. $^{15,17,20,22-24}$ We collected data on a single healthy user who interacted with the Novint Falcon while wearing IMU sensors strategically placed on her hand and forearm. We constructed a linear model that predicts the subject's wrist angles with exceptionally high accuracy. Analysis of the model's coefficients revealed that data from both the Novint Falcon and IMU sensors had strong predictive value. Intuitively, β_1 and Y were highly important to the model fit. The contribution of $\omega_{1,x}$ to the fit likely stemmed from ulnar pronation while the user interacted with the Novint Falcon, which indirectly led to changes in measured wrist angles.

In spite of the promising results, this work represents the first step in a greater endeavor. First, we will train the algorithm on data from additional users, to account for physiological and behavioral variability. Next, we will analyze out-of-sample error to ensure that the model we developed is generalizable to the majority of human users.²⁹ Finally, since our approach relies on "black box" machine learning, our methodology will greatly benefit from a physical model that relates the wrist angle to movement of the end-effector. Incorporating a physical model with biomechanical constraints could ultimately improve the interpretability of our model's predictions towards comprehensive, informed assessment by medical professionals.

ACKNOWLEDGMENTS

This study was funded by the National Science Foundation under grant numbers ECCS-1928614 and DUE-2129076.

REFERENCES

- [1] Virani, S. S., Alonso, A., Benjamin, E. J., Bittencourt, M. S., Callaway, C. W., Carson, A. P., Chamberlain, A. M., Chang, A. R., Cheng, S., Delling, F. N., et al., "Heart disease and stroke statistics—2020 update: A report from the american heart association," Circulation 141(9), e139-e596 (2020).
- [2] Carod-Artal, J., Egido, J. A., González, J. L., and Varela de Seijas, E., "Quality of life among stroke survivors evaluated 1 year after stroke: experience of a stroke unit," *Stroke* **31**(12), 2995–3000 (2000).
- [3] Squeri, V., Masia, L., Giannoni, P., Sandini, G., and Morasso, P., "Wrist rehabilitation in chronic stroke patients by means of adaptive, progressive robot-aided therapy," *IEEE Transactions on Neural Systems and Rehabilitation Engineering* 22(2), 312–325 (2013).
- [4] Prange, G. B., Jannink, M., Groothuis-Oudshoorn, C., Hermens, H. J., and IJzerman, M. J., "Systematic review of the effect of robot-aided therapy on recovery of the hemiparetic arm after stroke," (2009).

- [5] Carignan, C. R. and Krebs, H. I., "Telerehabilitation robotics: Bright lights, big future?," *Journal of Rehabilitation Research and Development* **43**(5), 695 (2006).
- [6] Maciejasz, P., Eschweiler, J., Gerlach-Hahn, K., Jansen-Troy, A., and Leonhardt, S., "A survey on robotic devices for upper limb rehabilitation," *Journal of Neuroengineering and Rehabilitation* 11(1), 1–29 (2014).
- [7] Hussain, S., Jamwal, P. K., Van Vliet, P., and Ghayesh, M. H., "State-of-the-art robotic devices for wrist rehabilitation: Design and control aspects," *IEEE Transactions on human-machine systems* **50**(5), 361–372 (2020).
- [8] Krebs, H. I., Volpe, B. T., Williams, D., Celestino, J., Charles, S. K., Lynch, D., and Hogan, N., "Robot-aided neurorehabilitation: a robot for wrist rehabilitation," *IEEE Transactions on Neural Systems and Rehabilitation Engineering* 15(3), 327–335 (2007).
- [9] Popescu, V. G., Burdea, G. C., Bouzit, M., and Hentz, V. R., "A virtual-reality-based telerehabilitation system with force feedback," *IEEE transactions on Information Technology in Biomedicine* **4**(1), 45–51 (2000).
- [10] Bouzit, M., Burdea, G., Popescu, G., and Boian, R., "The rutgers master ii-new design force-feedback glove," *IEEE/ASME Transactions on Mechatronics* **7**(2), 256–263 (2002).
- [11] Khor, K. X., Chin, P. J. H., Yeong, C. F., Su, E. L. M., Narayanan, A. L. T., Rahman, H. A., and Khan, Q. I., "Portable and reconfigurable wrist robot improves hand function for post-stroke subjects," *IEEE Transactions on Neural Systems and Rehabilitation Engineering* 25(10), 1864–1873 (2017).
- [12] Lambercy, O., Dovat, L., Gassert, R., Burdet, E., Teo, C. L., and Milner, T., "A haptic knob for rehabilitation of hand function," *IEEE Transactions on Neural Systems and Rehabilitation Engineering* **15**(3), 356–366 (2007).
- [13] Mandeljc, A., Rajhard, A., Munih, M., and Kamnik, R., "Robotic device for out-of-clinic post-stroke hand rehabilitation," *Applied Sciences* **12**(3), 1092 (2022).
- [14] Simpson, J., [Challenges and Trends Driving Telerehabilitation], 13–27, Springer London, London (2013).
- [15] Laut, J., Cappa, F., Nov, O., and Porfiri, M., "Increasing patient engagement in rehabilitation exercises using computer-based citizen science," *PLOS ONE* **10**(3), e0117013 (2015).
- [16] Li, K. F., Sevcenco, A.-M., and Yan, E., "Telerehabilitation using low-cost video game controllers," in [2013 Seventh international conference on complex, intelligent, and software intensive systems], 136–143, IEEE (2013).
- [17] Cappa, P., Clerico, A., Nov, O., and Porfiri, M., "Can force feedback and science learning enhance the effectiveness of neuro-rehabilitation? an experimental study on using a low-cost 3d joystick and a virtual visit to a zoo," *PLoS One* 8(12), e83945 (2013).
- [18] Martin, S. and Hillier, N., "Characterisation of the novint falcon haptic device for application as a robot manipulator," in [Australasian Conference on Robotics and Automation], 291–292, Citeseer (2009).
- [19] Coles, T. R. and John, N. W., "The effectiveness of commercial haptic devices for use in virtual needle insertion training simulations," in [Proceedings of the Third International Conference on Advances in Computer-Human Interactions], 148–153, IEEE (2010).
- [20] Panarese, A. and Edin, B. B., "A modified low-cost haptic interface as a tool for complex tactile stimulation," *Medical Engineering and Physics* **33**(3), 386–390 (2011).
- [21] Lin, Y. and Sun, Y., "5-d force control system for fingernail imaging calibration," in [Proceedings of the IEEE International Conference on Robotics and Automation], 1374–1379, IEEE (2011).
- [22] Lange, B., Flynn, S., and Rizzo, A., "Initial usability assessment of off-the-shelf video game consoles for clinical game-based motor rehabilitation," *Physical Therapy Reviews* **14**(5), 355–363 (2009).
- [23] Palsbo, S. E., Marr, D., Streng, T., Bay, B. K., and Norblad, A. W., "Towards a modified consumer haptic device for robotic-assisted fine-motor repetitive motion training," *Disability and Rehabilitation: Assistive Technology* 6(6), 546–551 (2011).
- [24] Scalona, E., Hayes, D., Palermo, E., Del Prete, Z., and Rossi, S., "Performance evaluation of 3d reaching tasks using a low-cost haptic device and virtual reality," in [Proceedings of the International Symposium on Haptic, Audio and Visual Environments Games], 1–5 (2017).

- [25] Kyberd, P. J., Lemaire, E. D., Scheme, E., MacPhail, C., Goudreau, L., Bush, G., and Brookeshaw, M., "Two-degree-of-freedom powered prosthetic wrist.," *Journal of Rehabilitation Research and Develop*ment 48(6) (2011).
- [26] Bajaj, N. M., Spiers, A. J., and Dollar, A. M., "State of the art in prosthetic wrists: Commercial and research devices," in [2015 IEEE International Conference on Rehabilitation Robotics], 331–338, IEEE (2015).
- [27] Barak-Ventura, R., Nakayama, S., Raghavan, P., Nov, O., and Porfiri, M., "The role of social interactions in motor performance: feasibility study toward enhanced motivation in telerehabilitation," *Journal of Medical Internet Research* 21(5), e12708 (2019).
- [28] Zeng, Y., Yang, J., Peng, C., and Yin, Y., "Evolving gaussian process autoregression based learning of human motion intent using improved energy kernel method of emg," *IEEE Transactions on Biomedical Engineering* **66**(9), 2556–2565 (2019).
- [29] Zhang, X., Cui, P., Xu, R., Zhou, L., He, Y., and Shen, Z., "Deep stable learning for out-of-distribution generalization," in [Proceedings of the IEEE/CVF Conference on Computer Vision and Pattern Recognition], 5372–5382 (2021).